

Aryl-Extended and Super Aryl-Extended Calix[4]pyrroles: Design, Synthesis, and Applications

Luis Escobar,* Qingqing Sun,* and Pablo Ballester*



Cite This: *Acc. Chem. Res.* 2023, 56, 500–513



Read Online

ACCESS |

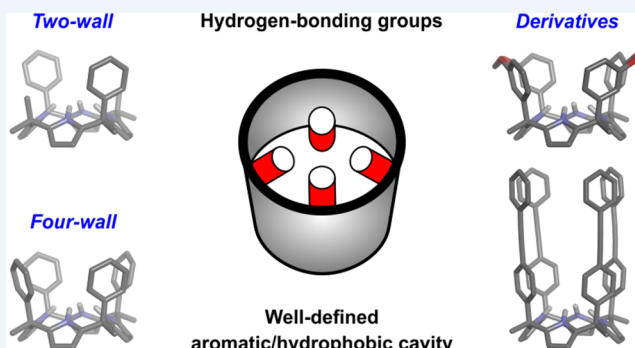
Metrics & More

Article Recommendations

CONSPECTUS: Proteins exhibit high-binding affinity and selectivity, as well as remarkable catalytic performance. Their binding pockets are hydrophobic but also contain polar and charged groups to contribute to the binding of polar organic molecules in aqueous solution. In the past decades, the synthesis of biomimetic receptors featuring sizable aromatic cavities equipped with converging polar groups has received considerable attention. “Temple” cages, naphthotubes, and aryl-extended calix[4]pyrroles are privileged examples of synthetic scaffolds displaying functionalized hydrophobic cavities capable of binding polar substrates. In particular, calix[4]pyrroles are macrocycles containing four pyrrole rings connected through their pyrrolic 2- and 5-positions by tetra-substituted sp^3 carbon atoms (*meso*-substituents). In 1996, Sessler introduced the *meso*-octamethyl calix[4]pyrrole as an outstanding receptor for anion binding. Independently, Sessler and Floriani also showed that the introduction of aryl substituents in the *meso*-positions produced aryl-extended calix[4]pyrroles as a mixture of configurational isomers. In addition, aryl-extended calix[4]pyrroles bearing two and four *meso*-aryl substituents (walls) were reported. The cone conformation of “two-wall” $\alpha\alpha$ -aryl-extended calix[4]pyrroles features an aromatic cleft with a polar binding site defined by four converging pyrrole NHs. On the other hand, “four-wall” $\alpha\alpha\alpha\alpha$ -calix[4]pyrrole isomers possess a deep polar aromatic cavity closed at one end by the converging pyrrole NHs. Because of their functionalized interior, aryl-extended calix[4]pyrroles are capable of binding anions, ion-pairs, and electron-rich neutral molecules in organic solvents. However, in water, they are restricted to the inclusion of neutral polar guests.

Since the early 2000s, our research group has been involved in the design and synthesis of “two-wall” and “four-wall” aryl-extended calix[4]pyrroles and their derivatives, such as aryl-extended calix[4]pyrrole cavitands and super aryl-extended calix[4]pyrroles. In this Account, we mainly summarize our own results on the binding of charged and neutral polar guests with these macrocyclic receptors in organic solvents and in water. We also describe the applications of calix[4]pyrrole derivatives in the sensing of creatinine, the facilitated transmembrane transport of anions and amino acids, and the monofunctionalization of bis-isocyanides. Moreover, we explain the use of calix[4]pyrrole receptors as model systems for the quantification of anion- π interactions and the hydrophobic effect. Finally, we discuss the self-assembly of dimeric capsules and unimolecular metallo-cages based on calix[4]pyrrole scaffolds. We comment on their binding properties, as well as on those of bis-calix[4]pyrroles having a fully covalent structure.

In molecular recognition, aryl-extended calix[4]pyrroles and their derivatives are considered valuable receptors owing to their ability to interact with a wide variety of electron-rich, neutral, and charged guests. Calix[4]pyrrole scaffolds have also been applied in the development of molecular sensors, ionophores, transmembrane carriers, supramolecular protecting groups and molecular containers modulating chemical reactivity, among others. We believe that the design of new calix[4]pyrrole receptors and the investigation of their binding properties may lead to promising applications in many research areas, such as supramolecular catalysis, chemical biology and materials science. We hope that this Account will serve to spread the knowledge of the supramolecular chemistry of calix[4]pyrroles among supramolecular and nonsupramolecular chemists alike.



KEY REFERENCES

- Adriaenssens, L.; Gil-Ramírez, G.; Frontera, A.; Quiñonero, D.; Escudero-Adán, E. C.; Ballester, P. Thermodynamic Characterization of Halide- π Interactions in Solution Using “Two-Wall” Aryl Extended Calix[4]pyrroles as Model System. *J. Am. Chem. Soc.*

Received: December 22, 2022

Published: February 3, 2023



2014, 136, 3208–3218.¹ This study reports the binding of halides to aryl-extended calix[4]pyrroles having electron-donating and electron-withdrawing groups at their meso-aryl substituents. The binding energies of the anion–π interaction in the complexes correlated with the molecular electrostatic potential of the receptors' aryl rings.

- Escobar, L.; Ballester, P. Quantification of the hydrophobic effect using water-soluble super aryl-extended calix[4]pyrroles. *Org. Chem. Front.* 2019, 6, 1738–1748.² This work describes the binding of pyridyl N-oxides, having nonpolar residues at the para-position, with super aryl-extended calix[4]pyrroles. The binding energies of the inclusion complexes and the surface area of the nonpolar residues enabled the quantification of the hydrophobic effect.
- Sierra, A. F.; Hernández-Alonso, D.; Romero, M. A.; González-Delgado, J. A.; Pischel, U.; Ballester, P. Optical Supramolecular Sensing of Creatinine. *J. Am. Chem. Soc.* 2020, 142, 4276–4284.³ This study reports the sensing of creatinine using an indicator displacement assay based on a fluorescent monophosphonate cavitand and a pyridyl N-oxide as a black-hole quencher. The displacement of the bound pyridyl N-oxide by creatinine produced a fluorescence turn-on sensor.
- Sun, Q.; Escobar, L.; Ballester, P. Hydrolysis of Aliphatic Bis-isocyanides in the Presence of a Polar Super Aryl-Extended Calix[4]pyrrole Container. *Angew. Chem., Int. Ed.* 2021, 60, 10359–10365.⁴ This work describes the application of a super aryl-extended calix[4]pyrrole in the monofunctionalization reaction of bis-isocyanides. The receptor acted as both a sequestering and supramolecular protecting group in the hydrolysis of bis-isocyanides, enhancing the reaction selectivity for the monoformamide products.

1. INTRODUCTION

In the past decades, molecular recognition using macrocyclic receptors has attracted considerable interest in supramolecular chemistry.⁵ Synthetic macrocycles aim to mimic the remarkable properties exhibited by biological receptors.^{6,7} They are synthesized by combining aromatic, aliphatic, and heterocyclic components. Some macrocycles possess internal cavities capable of surrounding the surface of the bound guest. Macrocyclic receptors have been used to investigate noncovalent interactions in solution.⁸ They have also found applications in molecular sensing,⁹ liquid–liquid extraction,¹⁰ transmembrane transport,¹¹ reactivity modulation,¹² and catalysis,¹³ among others.^{14,15}

Many macrocyclic receptors, i.e., calix[4]arene, resorcin[4]-arene, pillar[4]arene, cucurbit[n]uril, etc., feature aromatic cavities not functionalized with converging polar groups, which limits their use in binding processes exclusively relying on size and shape complementarity. High-affinity and selective binding of charged and neutral polar guests demands equipping the receptor's cavity with complementary functional/polar groups. Nevertheless, the synthesis of receptors possessing functionalized aromatic/hydrophobic cavities represents a challenging endeavor.^{16,17} We and others used calix[4]pyrrole (C[4]P) scaffolds to address the issue of functional complementarity for the binding of polar substrates.

In 1886, Baeyer¹⁸ reported the acid-catalyzed condensation of pyrrole with acetone to afford *meso*-octamethyl C[4]P 1 (Figure 1a). After being ignored for many years, 1 was reintroduced by Sessler as a privileged receptor for the binding of anions,¹⁹ ion-

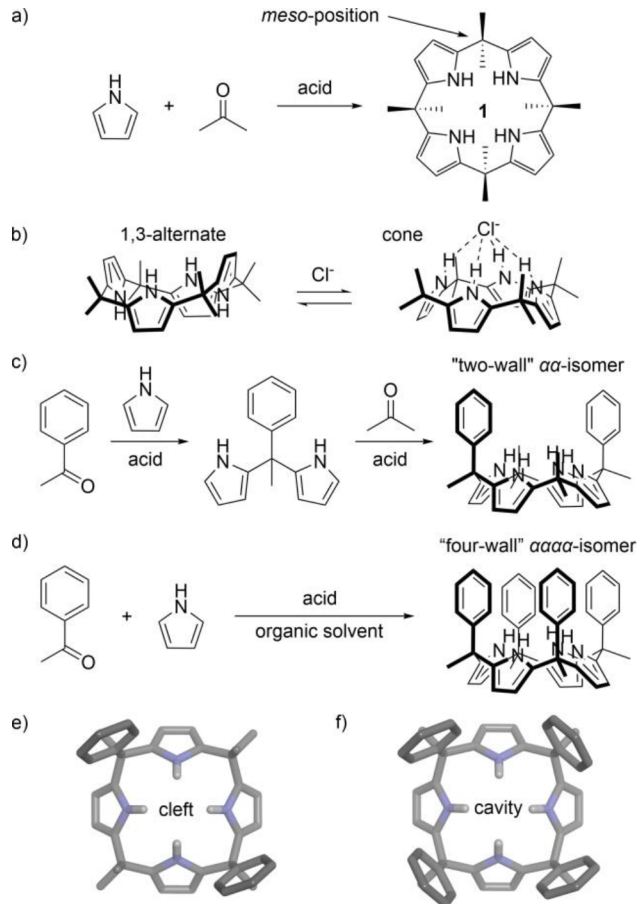


Figure 1. (a) Synthesis of 1. (b) Conformational change experienced by 1 upon chloride binding. Synthesis of (c) “two-wall” and (d) “four-wall” AE-C[4]Ps. Top views of the energy-minimized structures of (e) “two-wall” $\alpha\alpha$ - and (f) “four-wall” $\alpha\alpha\alpha\alpha$ -isomers.

pairs,^{20,21} and neutral polar molecules.²² In nonpolar solvents, 1 preferentially adopts 1,2- and 1,3-alternate conformations. The addition of a coordinating anion induces the switching of 1 into the cone conformation owing to the establishment of four convergent hydrogen bonds with the bound anion (Figure 1b). In addition, and mainly in nonpolar chlorinated solvents, 1 acts as ion-pair receptor in the complexation of cesium, imidazolium and alkylammonium salts of coordinating anions. The cation is included in the shallow and electron-rich aromatic cavity defined by the pyrrole rings of 1 in cone conformation. This cavity is opposite to the bound anion, and the included cation experiences favorable Coulombic, cation–π and CH–π interactions. This binding geometry is referred as receptor-separated ion-paired complex.²³

The substitution of two opposite *meso*-methyl groups in 1 by phenyl substituents provided “two-wall” aryl-extended calix[4]pyrroles (AE-C[4]Ps) (Figure 1c).²⁴ Analogously, the replacement of a methyl group in each one of the *meso*-carbons of 1 afforded “four-wall” AE-C[4]Ps (Figure 1d).^{25,26} The synthesis of “two-wall” AE-C[4]Ps involves two acid-mediated condensation reactions. First, the condensation of a methyl aryl ketone with pyrrole, used as solvent, affords a dipyrromethane. Second, the cyclocondensation of the obtained dipyrromethane with acetone, also used as solvent, gives the “two-wall” AE-C[4]P as a mixture of two configurational isomers: $\alpha\beta$ and $\alpha\alpha$, depending on the relative orientation of the two *meso*-aryl

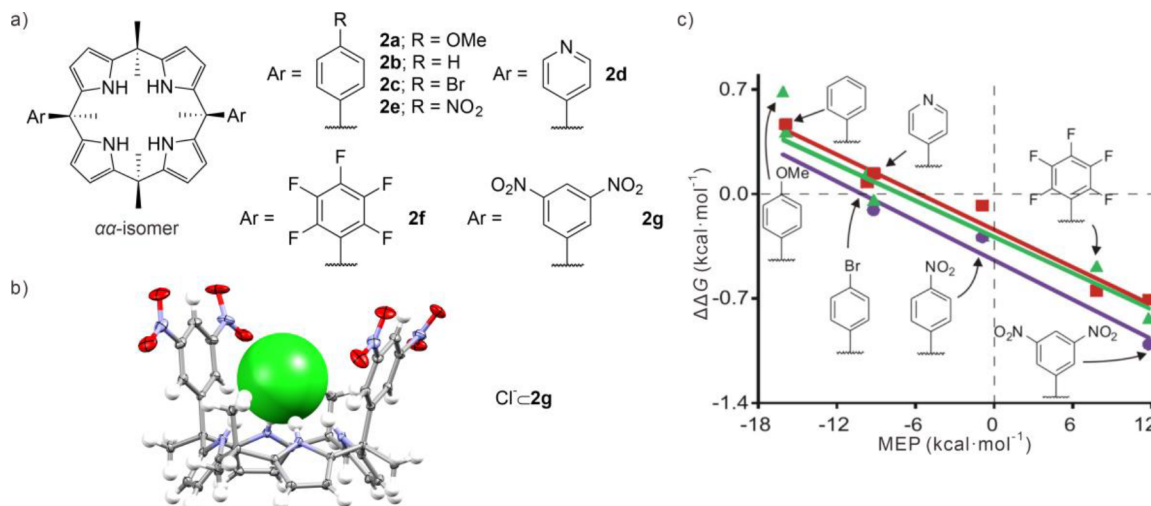


Figure 2. (a) Structures of **2a–g**. (b) X-ray structure of $\text{Cl}^- \cdot \text{2g}$ (CCDC-1002697). (c) Experimental values determined for the anion– π interaction of Cl^- (triangles), Br^- (squares), and I^- (circles) vs the calculated MEP values. Adapted with permission from ref 1. Copyright 2014 American Chemical Society.

substituents. For the same token, the direct acid-mediated cyclocondensation reaction of a methyl aryl ketone with pyrrole, in an organic solvent, produces crudes of “four-wall” AE-C[4]Ps containing up to four isomers: $\alpha\beta\alpha\beta$, $\alpha\alpha\beta\beta$, $\alpha\alpha\alpha\beta$, and $\alpha\alpha\alpha\alpha$ (or tetra- α). On the one hand, the cone conformation of the “four-wall” tetra- α isomer displays a deep aromatic cavity open at one end and equipped with a polar binding site at the closed end (Figure 1f). The tetra- α isomer is usually obtained in 5–20% yield in the cyclocondensation reaction, with some exceptions (e.g., >35% yield when using either *meta*- or *para*-hydroxyphenyl methyl ketones).^{25,27} On the other hand, the cone conformation of the “two-wall” $\alpha\alpha$ -isomer, which is usually produced in 5–30% yield upon the cyclocondensation step, presents an aromatic cleft with a polar binding site (Figure 1e). In both cases, the polar binding site is defined by four converging pyrrole NHs. The aromatic cavities/clefts of AE-C[4]Ps can be further elaborated by placing substituents at their upper rims.^{1–3} In addition, the *meso*-carbons of AE-C[4]Ps can bear alkyl substituents instead of methyl groups. For example, the cyclocondensation reaction to give “four-wall” AE-C[4]Ps bearing *meso*-alkyl substituents with terminal functional groups often fails or produces the tetra- α isomer in low yield (ca. 1%). Nevertheless, the use of methyltrialkylammonium chloride salts as templates enhances the macrocyclization reaction and favors the formation of the tetra- α isomer (up to 62% yield).²⁹ It is worth mentioning that the reaction conditions of the cyclocondensation in “two-wall” and “four-wall” AE-C[4]Ps lack of generality. They are dependent on the alkyl aryl ketone, acid and solvent used. Moreover, the macrocyclization reaction might suffer, in some cases, from low reproducibility.^{30,31}

Over the last 15 years, our research group focused on the design and synthesis of AE-C[4]P receptors for the selective and efficient binding of anions, ion-pairs, and neutral polar molecules. In this Account, we discuss the binding properties of “two-wall” and “four-wall” AE-C[4]Ps and their derivatives, such as AE-C[4]P cavitands and super aryl-extended C[4]Ps (SAE-C[4]Ps).³² We also describe their applications in molecular sensing, facilitated transmembrane transport, and modulation of chemical reactivity. Moreover, we demonstrate their use as model systems for the quantification of noncovalent interactions. Finally, we describe selected examples of bis-C[4]P

receptors based on covalent and self-assembled structures (dimeric capsules), as well as metallo-cages containing one C[4]P unit. We do not dwell in photoswitchable or mechanically interlocked receptors in this Account.

2. “TWO-WALL” ARYL-EXTENDED CALIX[4]PYRROLES

2.1. Anion Binding

“Two-wall” $\alpha\alpha$ -AE-C[4]Ps bind mono- and polyatomic anions through the establishment of four convergent hydrogen bonds between the pyrrole NHs and the anion.²⁴ Concomitantly, the receptor adopts the cone conformation sandwiching the anion between the two aromatic walls. This binding geometry forces the bound anion to directly interact with the π -systems of the *meso*-aryl substituents.³³

Taking advantage of the above binding geometry, we employed a series of “two-wall” AE-C[4]Ps, **2a–g** (Figure 2a), to determine the energetic contribution of anion– π interactions to the thermodynamic stability of their complexes with halides.¹ The *meso*-aryl substituents of **2a–g** were decorated with electron-donating and electron-withdrawing groups to tune their electronic characteristics. In acetonitrile, **2a–g** formed 1:1 anionic complexes (Figure 2b) with Cl^- , Br^- , and I^- (added as tetrabutylammonium (TBA^+) salts). The association constants (K_a) were determined using ¹H NMR spectroscopic titrations and isothermal titration calorimetry (ITC) experiments (Table 1).

Table 1. K_a Values (M^{-1}) of **1** and **2a–g** with Anions in Acetonitrile^{1,34}

receptors	anions			
	Cl^-	Br^-	I^-	NO_3^-
1	1.1×10^5	3.6×10^3	13	60
2a	1.1×10^4			
2b	2.6×10^4	8.0×10^2		30
2c	6.8×10^4	2.8×10^3		
2d	1.2×10^5	2.3×10^3	18	
2e	2.8×10^5	4.7×10^3	33	1.4×10^2
2f	5.5×10^5	3.2×10^4		7.1×10^2
2g	1.8×10^6	3.9×10^4	3.8×10^2	1.6×10^3

For any given receptor, the trend of thermodynamic stabilities of the complexes showed the order $\text{Cl}^- > \text{Br}^- > \text{I}^-$. This was due to the importance of electrostatic effects in charged hydrogen-bonding interactions. In addition, the binding affinities displayed by the receptors' series for a particular halide were dependent on the electronic properties of the *meso*-aryl substituents. For example, the K_a value determined for $\text{Cl}^- \subset 2\mathbf{g}$ was 2 orders of magnitude larger than that of $\text{Cl}^- \subset 2\mathbf{a}$. Moreover, only $\text{Cl}^- \subset 2\mathbf{f-g}$ were kinetically stable on the chemical shift time scale. This finding hinted at their superior thermodynamic stabilities.

We dissected the free energy component corresponding to the anion- π interactions by (a) considering that the contribution provided by the charged hydrogen-bonding interactions was constant in all complexes and (b) adjusting this value to the free energy calculated for $\text{X}^- \subset \mathbf{1}$. The free energies calculated for the anion- π interactions were obtained using the formula: $\Delta\Delta G_{\text{halide}-\pi} = (\Delta G_{\text{X}^- \subset 2} - \Delta G_{\text{X}^- \subset 1})/2$, the coefficient of 2 considers the presence of two aromatic walls and assumes that anion- π interactions are additive. The obtained $\Delta\Delta G_{\text{halide}-\pi}$ values displayed a linear relationship with the calculated molecular electrostatic potential (MEP) at the center of the aryl rings (Figure 2c). This result demonstrated that anion- π interactions became more favorable as the MEP value of the aryl ring turned more positive. For example, the interaction of Cl^- and Br^- with 1,3-dinitrobenzene was ca. $-0.7 \text{ kcal}\cdot\text{mol}^{-1}$. The interactions increased to $-1.0 \text{ kcal}\cdot\text{mol}^{-1}$ in the case of I^- , probably, due to the larger polarizability of this anion. The observed linear relationships demonstrated that the studied anion- π interactions were dominated by electrostatic effects.

2.2. Anion Transport

In collaboration with Matile, we investigated the strength of the anion- π interactions of NO_3^- using $\mathbf{2b}$ and $\mathbf{2e-g}$.³⁴ We also evaluated the transmembrane transport of anions facilitated by $\mathbf{2b}$ and $\mathbf{2e-g}$. In acetonitrile, the 1:1 anionic complexes of NO_3^- featured K_a values in the range of $10-10^3 \text{ M}^{-1}$ (Table 1) and experienced fast exchange binding dynamics on the chemical shift time scale. The X-ray structure of $\text{NO}_3^- \subset 2\mathbf{g}$ showed that only one of the oxygen atoms of the anion was hydrogen-bonded to the four pyrrole NHs of the receptor (Figure 3a). The bound NO_3^- was located almost perpendicular to the *meso*-aryl substituents of $\mathbf{2g}$ establishing anion- π interactions. For an alternative X-ray structure, see refs 34 and 35.

We explored the facilitated anion transport activity of $\mathbf{2b}$ and $\mathbf{2e-g}$ using large unilamellar vesicles composed of egg yolk phosphatidylcholine (EYPC). The transport process was monitored using the 8-hydroxy-1,3,6-pyrenetrisulfonate (HPTS) assay in HEPES buffered NaCl solution (pH 7.0). The obtained results indicated that $\mathbf{2e}$ and $\mathbf{2g}$ were the most active carriers in the transmembrane transport of NO_3^- featuring EC_{50} values (i.e., effective concentration needed to reach 50% activity) of 8.4 and 2.0 nM, respectively. In addition, $\mathbf{2e}$ and $\mathbf{2g}$ displayed an excellent selectivity for the transport of NO_3^- over other anions (Figure 3b,c). Notably, the transport activities of $\mathbf{2e}$ and $\mathbf{2g}$ were independent of the cation used in the experiments, suggesting that they operated via an anion/anion antiport mechanism.

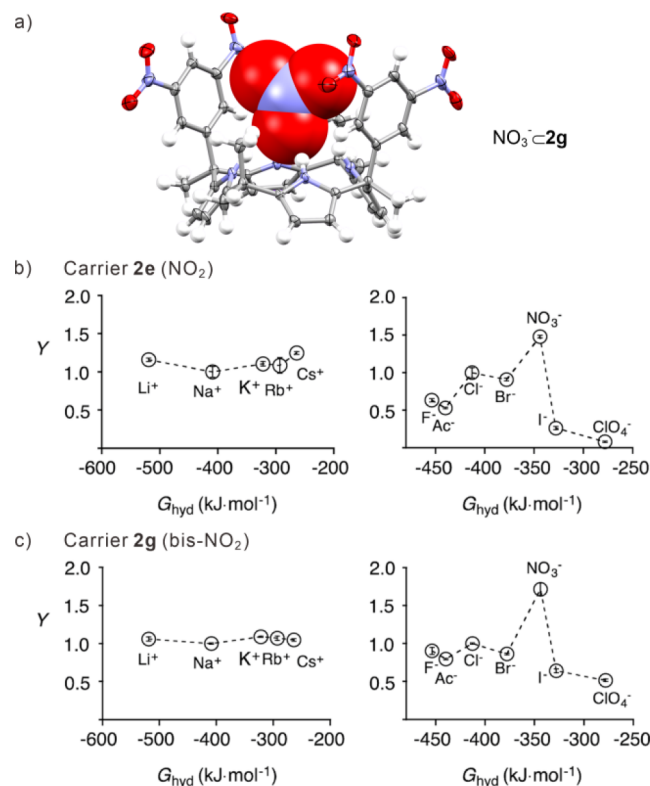


Figure 3. (a) X-ray structure of $\text{NO}_3^- \subset 2\mathbf{g}$ (CCDC-924961). Fractional transport activity ($Y = 1$ for Na^+Cl^-) of (b) $\mathbf{2e}$ and (c) $\mathbf{2g}$ using different cations (M^+Cl^-) and anions (Na^+A^-). Adapted with permission from ref 34. Copyright 2013 American Chemical Society.

3. “FOUR-WALL” ARYL-EXTENDED CALIX[4]PYRROLES

3.1. Anion Binding

The “four-wall” $\alpha\alpha\alpha\text{-AE-C}[4]\text{Ps}$ are also capable of binding anions through the formation of four convergent hydrogen bonds.²⁵ Consequently, the bound anion is surrounded by the four *meso*-aryl substituents of the receptor in cone conformation, leading to the establishment of multiple anion- π interactions.³³

We prepared a series of “four-wall” AE-C[4]Ps, $\mathbf{3a-f}$ (Figure 4a), and investigated the effect of chloride- π interactions on anion binding.³⁶ As before, the aromatic walls of $\mathbf{3a-f}$ were functionalized with different *para*-substituents in order to modify their electronic properties. We probed that, in acetonitrile, the binding of Cl^- to $\mathbf{3a-f}$ led to the formation of $\text{Cl}^- \subset \mathbf{3a-f}$ inclusion complexes (Figure 4b). In addition, all the complexes were kinetically stable on the chemical shift time scale. We determined that the K_a values of the complexes were in the range of 10^2-10^5 M^{-1} (Table 2). The magnitude of the K_a value was sensitive to the electronic nature of the *meso*-aryl substituents in $\mathbf{3a-f}$.

Using an analogous methodology to that described above for the “two-wall” counterparts, we calculated the binding energy deriving from the chloride- π interactions in $\text{Cl}^- \subset \mathbf{3a-f}$. The free energies assigned to the chloride- π interactions, $\Delta\Delta G_{\text{Cl}^--\pi} = (\Delta G_{\text{Cl}^- \subset 3} - \Delta G_{\text{Cl}^- \subset 1})/4$, correlated well with the Hammett constants of the receptors' *para*-substituents (Figure 4c). The calculated energy values showed that the chloride- π interaction was repulsive for $\text{Cl}^- \subset \mathbf{3a-e}$, whereas it was slightly attractive for $\text{Cl}^- \subset \mathbf{3f}$. These results also supported the conclusion that the chloride- π interaction was dominated by electrostatics. Note

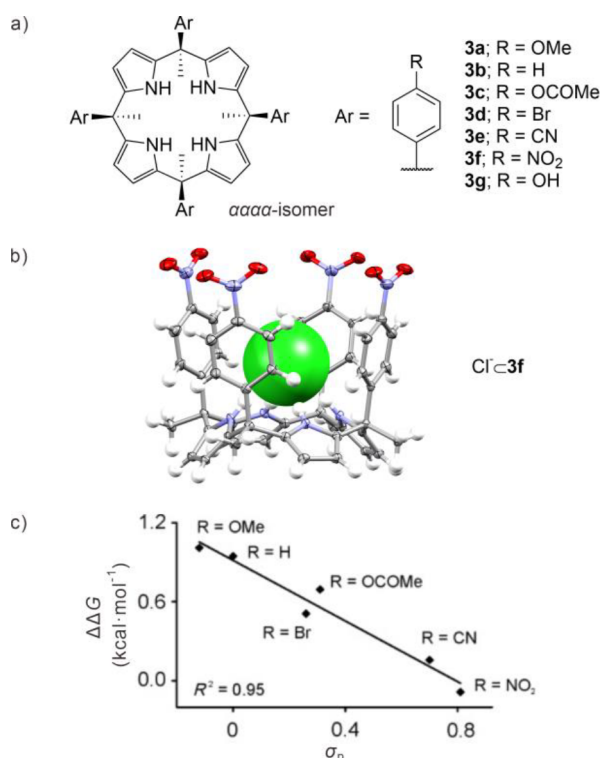


Figure 4. (a) Structures of 3a–g. (b) X-ray structure of $\text{Cl}^- \cdot 3\text{f}$ (CCDC-677143). (c) $\Delta\Delta G$ values determined for the chloride- π interactions vs the Hammett constants of the *para*-phenyl substituents. Adapted with permission from ref 36. Copyright 2008 Wiley.

Table 2. K_a Values (M^{-1}) of 3a–f with Chloride in Acetonitrile³⁶

receptors	anion	
	Cl ⁻	
3a	1.3×10^2	
3b	2.5×10^2	
3c	1.1×10^3	
3d	3.8×10^3	
3e	3.3×10^4	
3f	1.8×10^5	

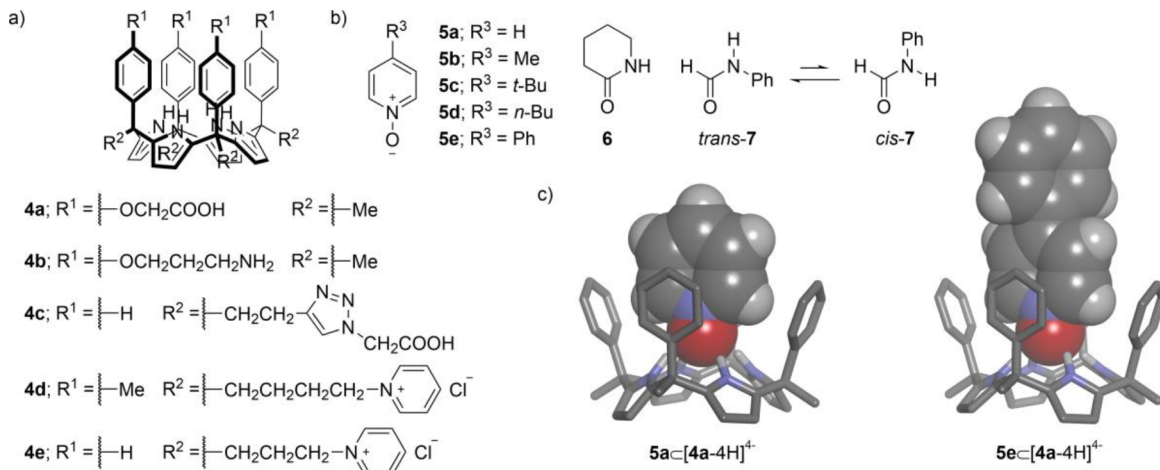


Figure 5. Structures of (a) 4a–e and (b) 5–7. (c) Energy-minimized structures of simplified $5\text{aC}[4\text{a}-4\text{H}]^{4+}$ and $5\text{eC}[4\text{a}-4\text{H}]^{4+}$.

that we did not use 3g in our studies on anion- π interactions in acetonitrile. However, Gale showed that ester and amide derivatives of 3g selectively bound F⁻ in dimethyl sulfoxide.³⁷

3.2. Molecular Recognition in Water

The synthesis of water-soluble “four-wall” *aaaa*-AE-C[4]Ps requires the incorporation of ionizable or charged groups at either the upper or lower rims.⁵ Their cone conformation displays a polar binding site buried in a deep hydrophobic cavity, which is suitable for the binding of neutral polar molecules in water. The included guest is stabilized by the hydrophobic effect (HE), hydrogen-bonding, $\pi-\pi$, and CH- π interactions.

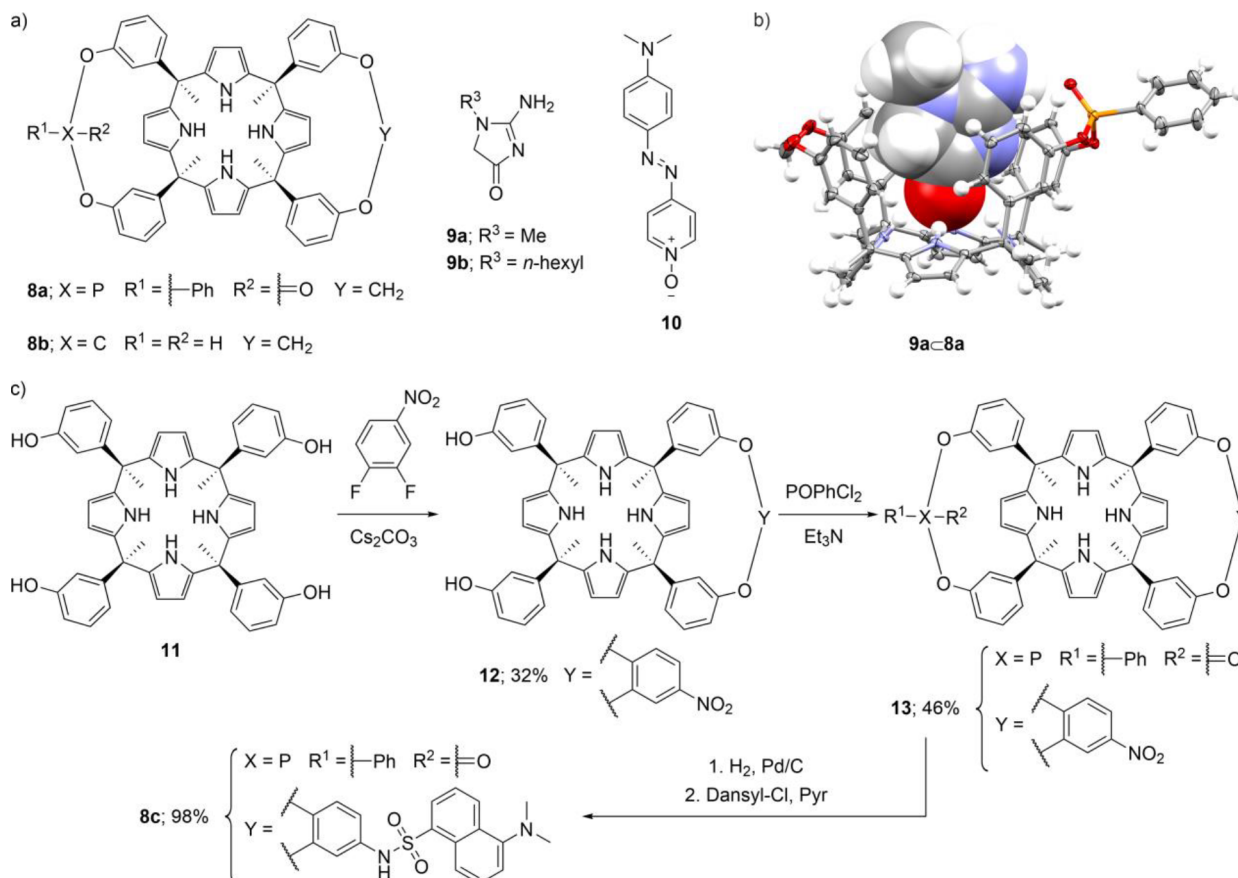
In 2009, we reported the first examples of water-soluble “four-wall” AE-C[4]Ps bearing terminal carboxylic acid and amino groups at the upper rim, 4a–b (Figure 5a).³⁸ Both compounds were soluble in water (pH ~ 7). We also studied the complexation of the pyridyl N-oxides 5a and 5e (Figure 5b) with 4a–b at pH ~ 7 using ¹H NMR and UV-vis spectroscopies. The AE-C[4]Ps, [4a-4H]⁴⁺ and [4b+4H]⁴⁺, formed thermodynamically and kinetically highly stable 1:1 inclusion complexes with 5a and 5e (Figure 5c). Although the receptors had an overall opposite charge, they displayed similar binding constants with the same guest (Table 3). On the contrary, the fact that the complexes of 5e were 1 order of magnitude less stable than those of 5a suggested the existence of steric clashes between the water-solubilizing groups and the *para*-phenyl substituent of 5e. Alternatively, the inclusion of 5e could have a negative effect in the solvation of the ionized terminal groups.

In this respect, we placed the water-solubilizing groups at the lower rim in 4c (Figure 5a).²⁸ On the one hand, the binding constants were similar for the complexes of 5a with both [4a-4H]⁴⁺ and [4c-4H]⁴⁺ (Table 3). On the other hand, 5eC[4c-4H]⁴⁺ was 2 orders of magnitude more stable than 5eC[4a-4H]⁴⁺.

Recently, we demonstrated that “four-wall” AE-C[4]Ps also bound cyclic and acyclic monoamides, such as 6 and 7 (Figure 5b and Table 3).^{39,40} For example, 4d⁴⁺ formed a thermodynamically highly stable 1:1 inclusion complex with 6. In addition, 4e⁴⁺ selectively bound *cis*-7 with high-binding affinity. This conformational selectivity was remarkable owing to the existence of free 7 in a 32:68 *cis/trans*-isomeric ratio. The binding of neutral polar guests to the polar hydrophobic cavity of water-soluble AE-C[4]Ps at room temperature (r.t.) was mainly

Table 3. K_a Values (M^{-1}) of 4a–e and 14a–b with 5–7 in Water^{2,28,38–40}

receptors	5a	5b	5c	5d	5e	6	cis-7	guests
[4a-4H] ⁴⁻	1.6×10^4					2.4×10^3		
[4b+4H] ⁴⁺	2.0×10^4					1.5×10^3		
[4c-4H] ⁴⁻	4.3×10^4					2.0×10^5		
4d ⁴⁺								7.1×10^4
4e ⁴⁺								$>10^4$
[14a-8H] ⁸⁻	8.6×10^5	2.0×10^6	9.1×10^6	1.0×10^8	1.2×10^9			
14b ⁸⁺	1.9×10^6	6.1×10^6	3.7×10^7	3.7×10^8	2.6×10^9			

**Figure 6.** (a) Structures of 8–10. (b) X-ray structure of 9a-C8a (CCDC-1431012). (c) Synthesis of 8c.

driven by enthalpy. This thermodynamic signature is characteristic of the so-called “non-classical” HE.⁵

4. ARYL-EXTENDED CALIX[4]PYRROLE CAVITANDS

We use the term “cavitand” in the case of “four-wall” AE-C[4]Ps featuring, at least, two adjacent *meso*-aryl substituents bridged. For binding studies of ion-pairs with phosphonate cavitands, see refs 41 and 42.

4.1. Recognition and Sensing of Creatinine

In 2016, we introduced the monophosphonate cavitand 8a for the selective and high-affinity binding of creatinine 9a (Figure 6a).²⁷ The concentration of creatinine in urine and plasma is a clinical biomarker of kidney performance and renal function, among others. By performing solid–liquid extraction experiments, we demonstrated that 8a extracted 1 equiv of the insoluble creatinine 9a into dichloromethane. The cavitand 8a included 9a in its polar aromatic cavity leading to the formation of 9a-C8a. The X-ray structure of 9a-C8a showed that the bound

creatinine established five hydrogen bonds with the cavitand (Figure 6b): four with the pyrrole NHs and one with the inwardly directed P=O group. The methylene protons of 9a were involved in CH–π interactions with two *meso*-aryl substituents. Based on the solubility of 9a ($<10^{-5} M$) and the quantitative formation of 9a-C8a, we estimated a $K_a > 10^7 M^{-1}$. The P=O group of 8a played an important role in the binding of 9a. In acetone, the monophosphonate cavitand 8a extracted 0.4 equiv of 9a, whereas the bis-methylene derivative 8b did not extract 9a, at least, at millimolar concentrations. Subsequently, we incorporated 8a in the sensing membrane of an ion-selective electrode (ISE). The cavitand 8a increased the sensitivity and selectivity of the ISE toward the detection of the creatininium cation, $[9a+H]^+$, in aqueous buffer solution and in bodily fluids.

Recently, we developed an indicator displacement assay (IDA) for hexyl creatinine 9b using the monophosphonate cavitand 8c, bearing a dansyl chromophore at the upper rim, and the pyridyl N-oxide 10 as quencher (Figure 6a).³ The synthesis

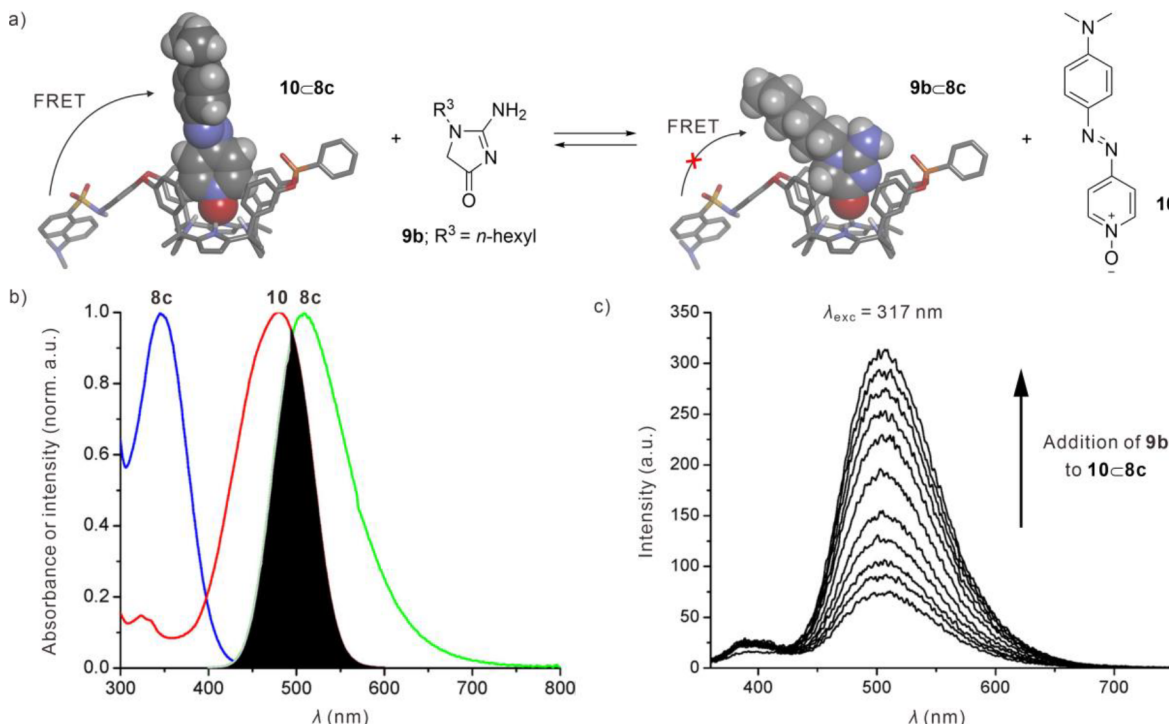


Figure 7. (a) Displacement of **10** in the IDA $10 \subset 8c$ by **9b**. (b) UV–vis absorption spectra of **8c** (blue) and **10** (red), and fluorescence spectrum of **8c** (green). Black area indicates spectral overlap. (c) Emission spectra for the IDA. Adapted with permission from ref 3. Copyright 2020 American Chemical Society.

of **8c** involved four reaction steps starting from the tetra-hydroxy AE-C[4]P **11** (Figure 6c). First, the nucleophilic aromatic substitution of 1,2-difluoro-4-nitrobenzene with **11** afforded the monoaryl-bridged intermediate **12**. Next, the monophosphonate mononitro cavitand **13** was obtained by reacting **12** with phenylphosphonic dichloride. Finally, the catalytic hydrogenation of **13**, followed by the coupling with dansyl chloride gave the monophosphonate cavitand **8c**. The inclusion of **10** in the cavity of **8c** led to the formation of $10 \subset 8c$ ($K_a = 1.2 \times 10^7 \text{ M}^{-1}$) and the quenching of the fluorescence of the dansyl chromophore by Förster resonance energy transfer (FRET) (Figure 7a,b). Next, the incremental addition of **9b** to the solution of $10 \subset 8c$ induced the displacement of **10** to the bulk solution and the formation of $9b \subset 8c$ ($K_a = 4.5 \times 10^5 \text{ M}^{-1}$). Accordingly, the competitive displacement of **10** by **9b** produced a fluorescence turn-on of the supramolecular sensor (Figure 7c). Similar results were obtained with **9a**.

4.2. Amino Acid Transport

We demonstrated that **8a** was also able to extract L-Pro into dichloromethane owing to the formation of a 1:1 inclusion complex ($K_a > 10^6 \text{ M}^{-1}$) (Figure 8a).⁴³ Based on this result, we applied **8a** as a molecular carrier to facilitate the transport of amino acids across liposomal and human HeLa cell membranes.

Using a radiometric assay and [³H]-radiolabeled amino acids, we observed that **8a** facilitated the transport of L-Pro across liposomal membranes (0.1% carrier/EYPC) in HEPES buffer (pH 7.4) (Figure 8b). In addition, **8a** displayed a remarkable selectivity for the facilitated transport of L-Pro over other amino acids (Figure 8c). In human HeLa cell membranes, **8a**, embedded in the membrane of 1-palmitoyl-2-oleoyl-sn-glycero-3-phosphocholine (POPC) liposomes (10% carrier/POPC), contributed to the cellular uptake of L-Pro, in combination with that mediated by the natural transporters.

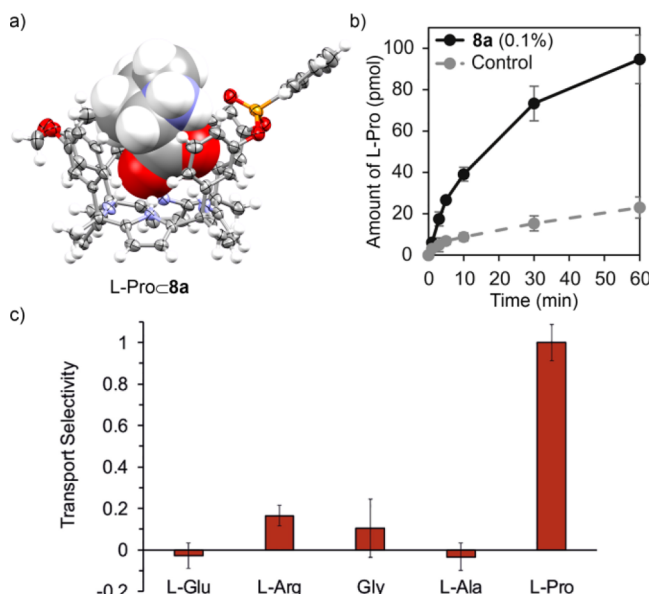


Figure 8. (a) X-ray structure of L-Pro**8a** (CCDC-1984688). (b) Time-course plots of the facilitated transport experiment of L-Pro using liposomes incorporating **8a** and control experiments. (c) Transport selectivity (selectivity = 1 for L-Pro) for different amino acids using **8a**. Adapted with permission from ref 43. Copyright 2020 Elsevier.

5. SUPER ARYL-EXTENDED CALIX[4]PYRROLES

We introduced “four-wall” $\alpha\alpha\alpha\alpha$ -SAE-C[4]Ps in 2016.⁴⁴ Their synthesis involved the attachment of *para*-ethynyl-aryl substituents at the upper rim of “four-wall” $\alpha\alpha\alpha\alpha$ -AE-C[4]Ps. In cone conformation, SAE-C[4]Ps feature a deeper and more hydrophobic aromatic cavity than the parent AE-C[4]Ps.

5.1. Quantification of the Hydrophobic Effect

In water, the HE is mainly responsible of the high-binding affinities shown by biological and synthetic supramolecular complexes.⁵ Polar interactions provide binding selectivity. In this sense, we assessed the HE exerted by the inclusion of nonpolar residues in the aromatic/hydrophobic cavity of water-soluble SAE-C[4]Ps.

We prepared two SAE-C[4]Ps, **14a–b** (Figure 9a), bearing eight ionizable or charged groups placed at the terminal positions of the four *meso*-aryl and the four *meso*-alkyl substituents.² Briefly, the quadruple Sonogashira cross-coupling reactions of the tetra-iodo AE-C[4]Ps **15a–b** with the *para*-

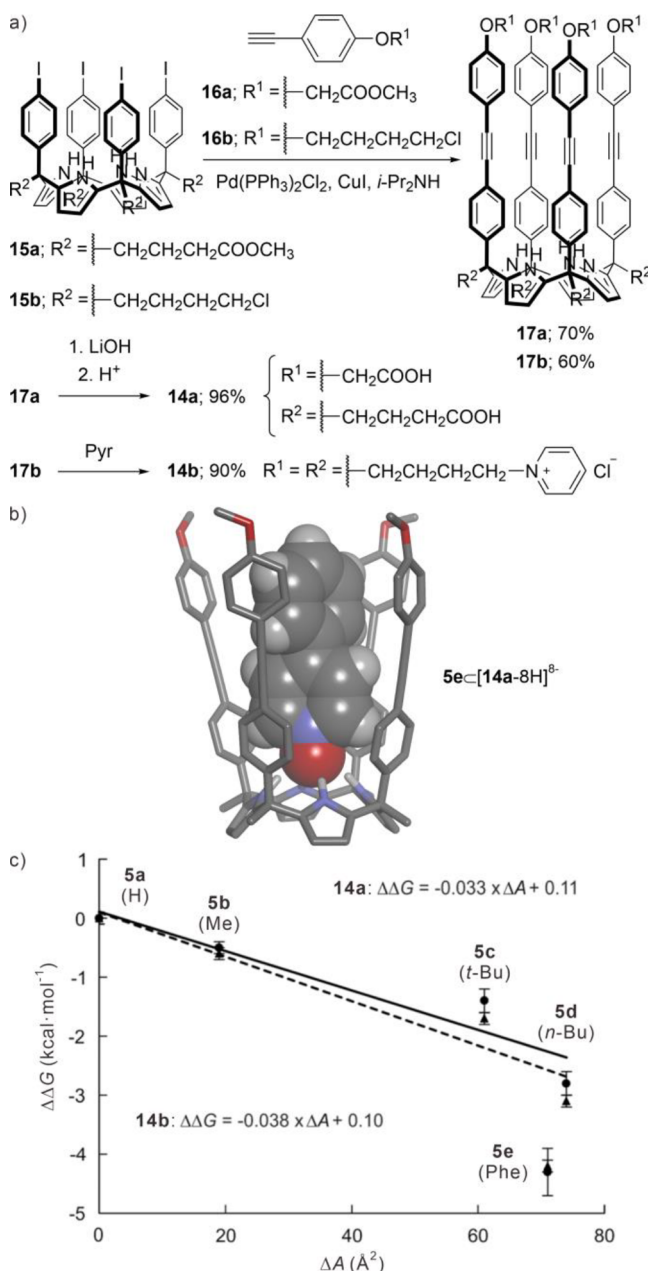


Figure 9. (a) Synthesis of **14a–b**. (b) Energy-minimized structure of simplified **5e**–**[14a-8H]⁸⁻**. (c) Differences in free energy vs *para*-substituent's surface area for the complexes of **14a** (circles) and **14b** (triangles). Adapted with permission from ref 2. Copyright 2019 Royal Society of Chemistry.

ethynyl-aryl compounds **16a–b** afforded the octa-ester and the octa-chloro SAE-C[4]Ps **17a–b**. The octa-ester **17a** was hydrolyzed with LiOH, obtaining the octa-acid derivative **14a**. In turn, the octa-pyridinium **14b** was prepared by heating the parent octa-chloro **17b** in pyridine. In water, **14a** was soluble at pH ~ 10, whereas **14b** was soluble at any pH. Both SAE-C[4]Ps, [**14a**–8H]⁸⁻ and **14b**⁸⁺, displayed sharp and well-defined proton signals in the bound form, i.e., when locked in cone conformation. Next, we determined the binding constants of **14a–b** with a series of pyridyl N-oxides, having a nonpolar *para*-substituent, **5b–e** (Figure 5b). Both SAE-C[4]Ps formed 1:1 inclusion complexes with the guests. The pair of complexes with the same guest featured similar *K_a* values and followed the order **5b** < **5c** < **5d** < **5e** (Table 3). These results indicated that the increase in the surface area of the *para*-substituent translated into a gain in binding affinity.

Considering that the interaction of the pyridyl N-oxide residue was constant throughout the guests' series and using **5a** as a reference, we calculated the binding energy, ΔΔG, derived from the inclusion of the nonpolar *para*-substituent of **5b–e** in the cavity of [**14a**–8H]⁸⁻ and **14b**⁸⁺. For each receptor, the calculated energy values displayed a linear relationship with the surface area of the *para*-substituents (Figure 9c). In these model systems, the HE was determined to be 33–38 cal·mol⁻¹·Å⁻². Although the surface areas of the *para*-substituents of **5d–e** were similar, the complexes of **5e** were stabilized by an additional 2 kcal·mol⁻¹, possibly, owing to the formation of multiple aromatic interactions at the upper rim of the SAE-C[4]Ps (Figure 9b).

5.2. Monofunctionalization of Aliphatic Bis-isocyanides

The monofunctionalization of symmetric difunctional compounds having independent reacting groups yields statistical mixtures of products. Among others, macrocyclic receptors have been used to improve the reaction selectivity toward the monofunctionalized product.¹² For example, the acid-catalyzed hydrolysis of aliphatic bis-isocyanides **18a–c** yields statistical mixtures containing starting materials, monoformamides **19a–c** and bis-formamides **20a–c** (Figure 10a). Based on our previous knowledge on the binding of formamides to AE-C[4]Ps,³⁹ we addressed the monofunctionalization problem of **18a–c** using **14b**.⁴

First, we characterized the 1:1 inclusion complexes of **14b**⁸⁺ with **18–20** in water. For instance, the complexes of the guests having five methylene spacer groups featured *K_a* (**18b**–**14b**⁸⁺) = 1.3×10^5 M⁻¹, *K_{app}* (**19b**–**14b**⁸⁺) = 6.9×10^5 M⁻¹ and *K_{app}* (**20b**–**14b**⁸⁺) = 9.2×10^5 M⁻¹ at 313 K. The alkyl chain of the included guests adopted a fully extended conformation. The nonsymmetric guest **19b**, once included within **14b**⁸⁺, displayed the *cis*-formamide end bound to the C[4]P unit, whereas the isonitrile end was placed close to the open rim of the receptor (Figure 10b). Next, we studied the acid-catalyzed hydrolysis, at 313 K, of **18a–c** (Figure 10c). In the absence of **14b**⁸⁺, the reaction yielded **19a–c** in a maximum amount of 50% after 20 min. Considering two irreversible reactions, we calculated $k_1 = 7.0 \times 10^{-2}$ min⁻¹ and $k_2 = 3.5 \times 10^{-2}$ min⁻¹. In contrast, in the presence of 1 equiv of **14b**⁸⁺, the reaction yielded a mixture of nonstatistical composition and displayed a decrease in reaction rates. For the bis-isonitrile **18b**, the monohydrolyzed product **19b** reached a maximum amount of 80% after 2 h. The kinetic data fit well to a model that considered two irreversible reactions (k_1 and k_2) and the reversible formation of the three complexes (*K_a* [**18b**–**14b**⁸⁺], *K_{app}* [**19b**–**14b**⁸⁺], and *K_{app}* [**20b**–**14b**⁸⁺]).

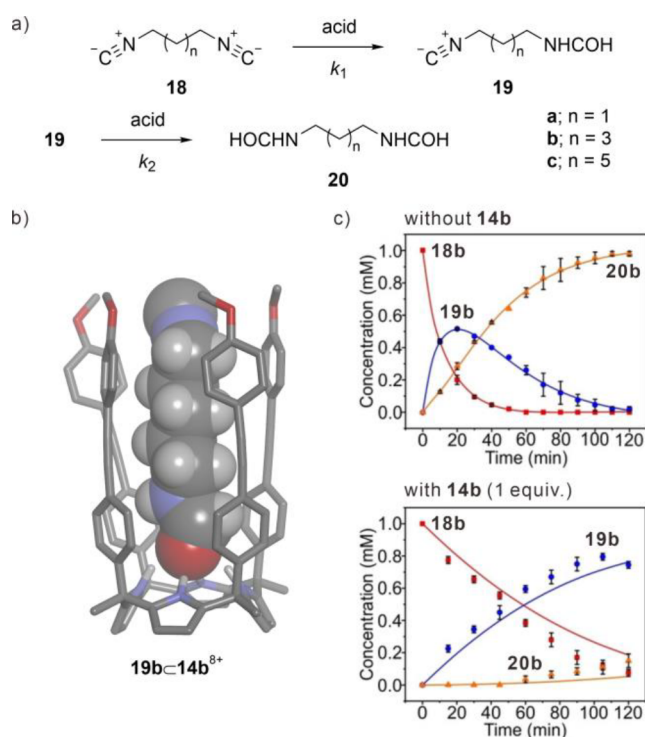


Figure 10. (a) Acid-catalyzed hydrolysis of **18a–c**. (b) Energy-minimized structure of simplified $19b\subset 14b^{8+}$. (c) Plots of concentrations vs time for the reaction of **18b** in the absence/presence of **14b**. Adapted with permission from ref 4. Copyright 2021 Wiley.

This result demonstrated that $14b^{8+}$ functioned as both, a sequestering and supramolecular protecting group, enhancing the selectivity of the reaction for **19b**.

For the shorter bis-isocyanide **18a**, the selectivity for **19a** was reduced to 70% owing to the decrease in the thermodynamic stability of $19a\subset 14b^{8+}$. For the longer bis-isocyanide **18c**, the monoformamide **19c** reached a maximum amount of 55%. Although $18c/19c\subset 14b^{8+}$ were thermodynamically highly stable, one isocyanide group protruded into the water/receptor interface.

6. COVALENT “TWO-WALL” BIS-CALIX[4]PYRROLES

6.1. Design and Synthesis

The covalent linkage of two $\alpha\alpha$ -C[4]P units through their *para*-positions provided “two-wall” bis-C[4]Ps. Two different approaches are described in the literature for their syntheses.⁴⁵ One of them consists on directly coupling two identical or not $\alpha\alpha$ -disubstituted C[4]Ps. Following this approach, we synthesized **21a–b** bearing 1,3-diyne and 1,4-triazole linkers, respectively (Figure 11).^{46,47} It is worth mentioning that the efficient synthesis of **21b** required the use of tetrabutylammonium terephthalate as template. The other approach involves the condensation of two identical bis-dipyrromethane units with acetone.^{48,49}

6.2. Anion Binding and Cooperative Effects

The bis-C[4]Ps **21a–b** can bind simultaneously two ion-pairs leading to the formation of 1:2 complexes.⁴⁵ The influence of the first guest binding, i.e., formation of a 1:1 complex ($K_{1:1}$), on the binding affinity for the second guest ($K_{1:2}$) can be assessed using the cooperativity factor: $\alpha = 4 \times K_{1:2}/K_{1:1}$. Based on this

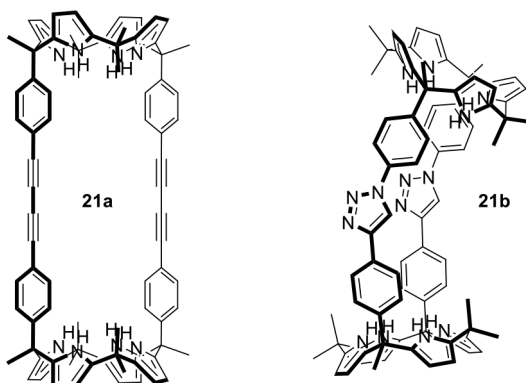


Figure 11. Structures of **21a–b**.

relationship, a binding process of two ion-pairs can display positive ($\alpha > 1$), negative ($\alpha < 1$), or no-cooperativity ($\alpha = 1$).

We investigated the interaction of **21a** with TBA⁺OCN[−], TBA⁺Cl[−], and methyltriptyl ammonium chloride (MTOA⁺Cl[−]) in chloroform.⁵⁰ For the TBA⁺ salts, **21a** established 1:2 cascade complexes featuring an included ion-triplet in close-contact binding mode (Figure 12a). This binding

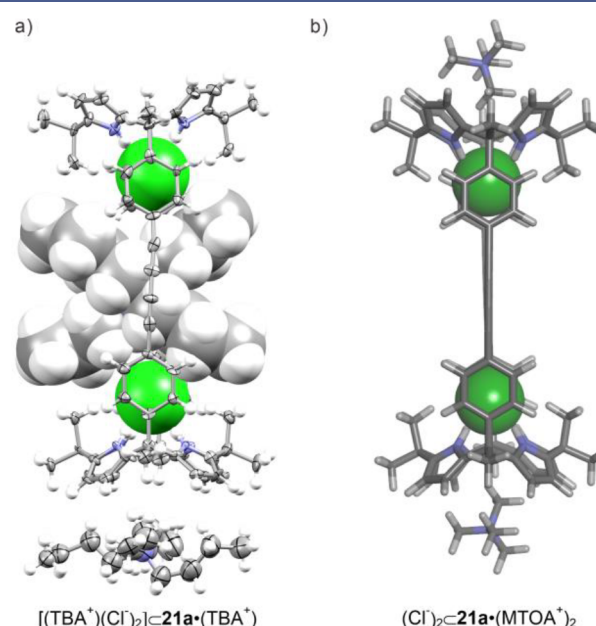


Figure 12. (a) X-ray structure of $[(TBA^+)(Cl^-)]_2 \subset 21a \cdot (TBA^+)$ (CCDC-930894). (b) Energy-minimized structure of simplified $(Cl^-)_2 \subset 21a \cdot (MTOA^+)_2$.

geometry produced a large positive cooperativity in the second binding event (Table 4). In turn, the 1:2 complex of the MTOA⁺ salt featured a receptor-separated binding geometry for the two

Table 4. K_a Values ($K_{1:1} \times K_{1:2}, M^{-2}$) and α (in Parentheses) of the 1:2 Complexes of Ion-Pairs with **21a–b**^{47,50}

receptors	ion-pairs		
	TBA ⁺ OCN [−]	TBA ⁺ Cl [−]	MTOA ⁺ Cl [−]
21a	1.5×10^{11} (1.3×10^8)	1.9×10^9 (1.9×10^7)	2.4×10^9 (35)
21b	6.8×10^8 (4)	5.3×10^7 (4)	4.0×10^{10} (4.0×10^{-2})

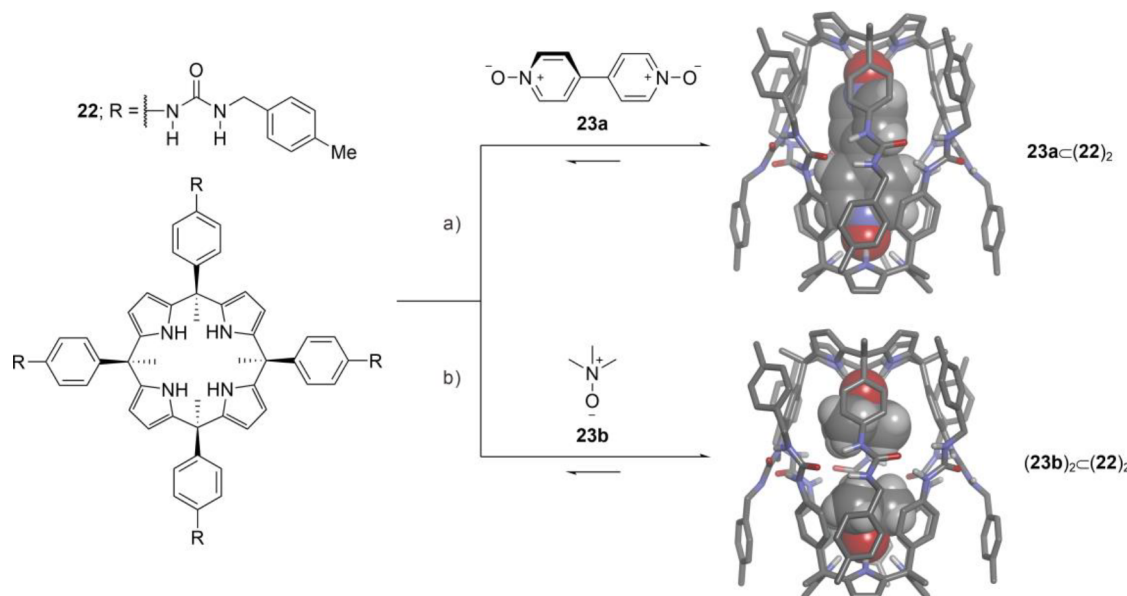


Figure 13. Structure of 22. Energy-minimized structures of (a) $23\text{a}\subset(22)_2$ and (b) $(23\text{b})_2\subset(22)_2$.

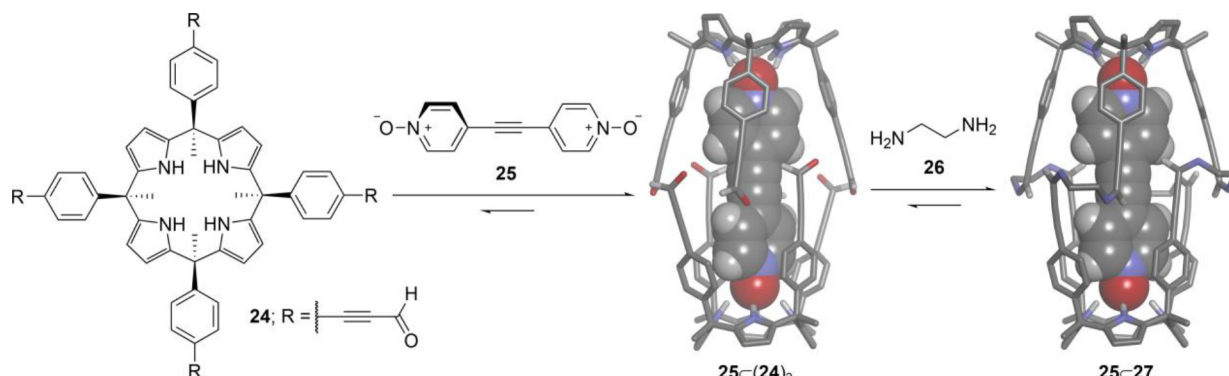


Figure 14. Structure of 24. Energy-minimized structures of $25\subset(24)_2$ and $25\subset 27$.

ion-pairs (Figure 12b). For this reason, the cooperativity factor in $(\text{Cl}^-)_2\subset 21\text{a}\cdot(\text{MTOA}^+)_2$ was much lower than for the TBA⁺ salt.

We also assessed the binding cooperativity of the same ion-pairs with 21b.⁴⁷ Although the geometries of the 1:2 complexes of 21b were identical with those described above for 21a, its binding cooperativity was negative in the case of MTOA⁺Cl⁻ (possibly anion repulsion due to the smaller cavity) and null for the TBA⁺ salts (inadequate size for sandwiching the cation between the two bound anions).

7. DIMERIC CAPSULES ASSEMBLED FROM "FOUR-WALL" CALIX[4]PYRROLES

"Four-wall" AE-C[4]Ps equipped with suitable functional groups at their upper rims self-assemble into dimeric capsules by establishing intermolecular hydrogen-bonding interactions.⁵¹ They are also used for the self-assembly of dynamic covalent cages and capsules. These supramolecular architectures present persistent polar cavities controlling the relative position and orientation of the included guests.⁵²

7.1. Hydrogen-Bonded Capsules

Sessler²⁵ and Floriani²⁶ reported the first examples of hydrogen-bonded capsules assembled in the solid-state from 3g (Figure 4a). This AE-C[4]P also formed sodium and pH responsive

hydrogels in the presence of the tetramethylammonium cation (TMA⁺).⁵³ Subsequently and inspired by the works of Rebek⁵⁴ and Böhmer,^{55,56} we investigated the dimerization of tetra-urea 22 (Figure 13a,b).⁵⁷ In dichloromethane and in the presence of 0.5 equiv of 23a, 22 self-assembled quantitatively into a dimeric capsule including one molecule of 23a ($K_a > 10^8 \text{ M}^{-2}$). The encapsulated 23a established hydrogen bonds with the two polar ends of (22)₂. Moreover, the urea groups of (22)₂ were unidirectionally oriented and formed a cyclic array of 16 hydrogen bonds.

We also demonstrated the pairwise encapsulation of guests in (22)₂. For example, a 1:1 mixture of 22 and 23b self-assembled quantitatively into (23b)₂C(22)₂.⁵⁸ In addition, a 2:1:1 mixture of 22, 23b, and MTOA⁺Cl⁻ in chloroform produced exclusively [(23b)(Cl⁻)₂C(22)₂(MTOA⁺)].⁵⁹ The included 23b and Cl⁻ occupied the polar ends of (22)₂ with a chloroform molecule sandwiched between them.

7.2. Dynamic Covalent Capsules

We used dynamic covalent chemistry for the self-assembly of tetra-aldehyde 24 in a capsular dimer (Figure 14).⁶⁰ In chloroform, the combination of 24 with 0.5 equiv of 25 induced the quantitative self-assembly of 25C(24)₂. In the complex, the formyl groups of 24 established a cyclic array of 8 hydrogen bonds and displayed a suitable arrangement for a subsequent

interhemisphere imine condensation reaction with selected diamines. The addition of 4 equiv of **26** to the solution of **25C(24)₂** afforded the octa-imine **25C27**.

Recently, we assembled a tetra-imine cage by direct condensation of **24** with a tetra-amine AE-C[4]P.⁶¹ In this case, a templating guest was not required for the formation of the cage in chloroform, yet the addition of 10% acetonitrile or 1 equiv of **23a** increased the reaction yield.

8. UNIMOLECULAR METALLO-CAGES BASED ON SUPER ARYL-EXTENDED CALIX[4]PYRROLES

8.1. Design and Self-Assembly

In order to preorganize SAE-C[4]Ps in cone conformation and fully close their aromatic cavities, we studied the self-assembly of coordination cages (CCs) using M(II) (M = Pd,Pt) metal centers and SAE-C[4]Ps bearing four *meta*-pyridyl units at the upper rim, **28a–b** (Figure 15a).^{62,63} In 2:1 chloroform/

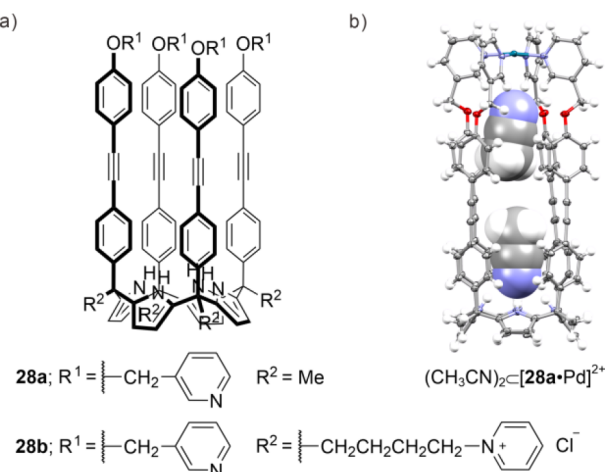


Figure 15. (a) Structures of **28a–b**. (b) X-ray structure of $(\text{CH}_3\text{CN})_2\subset[\text{28a}\cdot\text{Pd}]^{2+}$ (CCDC-1876530).

acetonitrile, **28a** adopted the cone conformation by binding an acetonitrile molecule. The addition of 1 equiv of $[\text{M}(\text{CH}_3\text{CN})_4](\text{BF}_4)_2$, followed by thermal equilibration induced the self-assembly of a monometallic CC, $[\text{28a}\cdot\text{M}]^{2+}$ (Figure 15b). The X-ray structure of $[\text{28a}\cdot\text{Pd}]^{2+}$ showed that the coordination of Pd(II) provided an additional polar binding site defined by four inwardly directed α -pyridyl protons. Two encapsulated acetonitrile molecules filled the CC's cavity and complemented the hydrogen-bonding needs of the two opposed polar binding sites.

We also attached four pyridinium residues at the lower rim in **28b**.⁶⁴ In the presence of suitable polar guests, **28b** and Pd(II) (added as NO_3^- salt) self-assembled into a water-soluble CC, $[\text{28b}\cdot\text{Pd}]^{6+}$. In water, the CC experienced significant aggregation at r.t., which was reduced by heating the solution at 333 K.

8.2. Encapsulation of Neutral Polar Guests

The CCs, $[\text{28a–b}\cdot\text{M(II)}]$, encapsulated mono- and ditopic polar guests (Figure 16a–d).^{62–64} Monotopic guests were bound to the binding site defined by the C[4]P unit and partially filled the CC's cavity. In these cases, the coencapsulation of an acetonitrile or water molecule was mandatory. The solvent molecule was hydrogen-bonded to the pyridyl α -CHs and assisted in the ideal 55% filling of the cavity volume. In contrast, ditopic guests complemented the hydrogen-bonding requests of

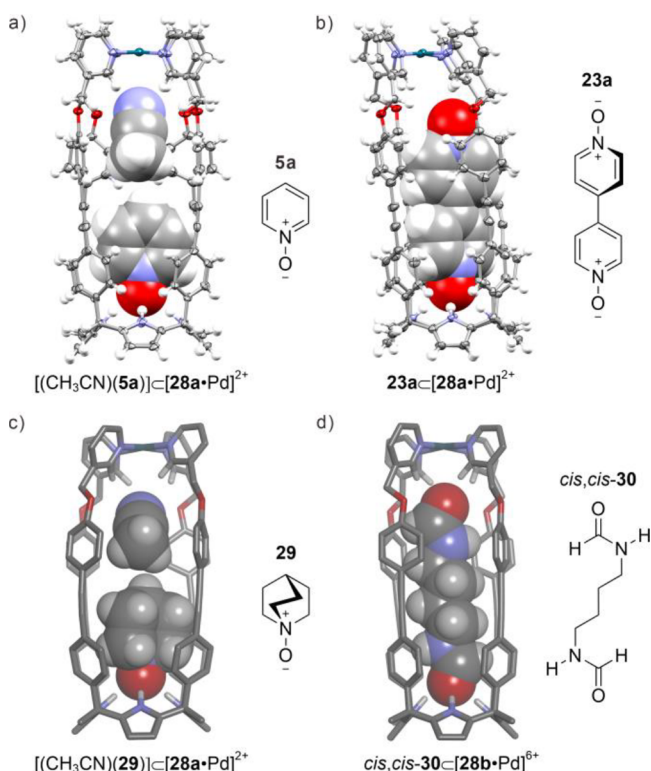


Figure 16. X-ray structures of (a) $[(\text{CH}_3\text{CN})(\text{5a})]\subset[\text{28a}\cdot\text{Pd}]^{2+}$ (CCDC-1876528) and (b) $23a\subset[\text{28a}\cdot\text{Pd}]^{2+}$ (CCDC-1876529). Energy-minimized structures of (c) $[(\text{CH}_3\text{CN})(\text{29})]\subset[\text{28a}\cdot\text{Pd}]^{2+}$ and (d) simplified *cis,cis*-**30** $\subset[\text{28b}\cdot\text{Pd}]^{6+}$.

both binding sites and filled completely (55%) the CC's cavity volume.

In 2:1 chloroform/acetonitrile, the addition of **5a** or **23a** to $[\text{28a}\cdot\text{Pd}]^{2+}$ led to the quantitative formation of $[(\text{CH}_3\text{CN})\cdot(\text{5a})]\subset[\text{28a}\cdot\text{Pd}]^{2+}$ and $23a\subset[\text{28a}\cdot\text{Pd}]^{2+}$, respectively.⁶² Similarly, the addition of **29** to $[\text{28a}\cdot\text{Pd}]^{2+}$ produced $[(\text{CH}_3\text{CN})\cdot(\text{29})]\subset[\text{28a}\cdot\text{Pd}]^{2+}$ ($K_a = 5 \times 10^3 \text{ M}^{-1}$).⁶³ In water, $[\text{28b}\cdot\text{Pd}]^{6+}$ also encapsulated **5a** and **23a**.⁶⁴ Moreover, $[\text{28b}\cdot\text{Pd}]^{6+}$ showed high-conformational selectivity by exclusively binding *cis,cis*-**30** ($K_a > 10^5 \text{ M}^{-1}$).

9. CONCLUSION AND PERSPECTIVE

We reviewed our own results on the supramolecular chemistry of AE-C[4]Ps and their derivatives. In solution, C[4]Ps were shown to bind anions, ion-pairs, and neutral polar molecules. The binding studies of halides with “two-wall” and “four-wall” AE-C[4]Ps provided experimental energy values for gauging anion-π interactions. The elaboration of the aromatic cavity of “four-wall” AE-C[4]Ps afforded AE-C[4]P cavitands and SAE-C[4]Ps. AE-C[4]Ps acted as carriers in the facilitated transmembrane transport of anions (“two-wall” AE-C[4]Ps) but also of amino acids (cavitands). Monophosphonate cavitands were also employed for the recognition and sensing of creatinine. The placement of ionizable or charged groups at the periphery of “four-wall” AE- and SAE-C[4]Ps enabled to study molecular recognition processes in water. Water-soluble SAE-C[4]Ps were used for the quantification of the HE and the monofunctionalization reaction of bis-isonitriles. The upper rim elaboration of AE- and SAE-C[4]Ps enabled the covalent construction of bis-C[4]Ps and the self-assembly of dimeric capsules and unimolecular metallo-cages.

Other authors implemented C[4]Ps in supramolecular¹⁴ and covalent^{65,66} polymeric materials (anion capture) and in therapeutics (potential anticancer drugs).¹⁵ In addition, “two-wall” AE-C[4]Ps and cavitand derivatives described here might find potential applications as therapeutic tools owing to their transmembrane transport properties. Moreover, the functionalization of surfaces with AE-C[4]P derivatives might lead to the development of sensors. However, the practical applications of AE- and SAE-C[4]Ps require increasing the yields of the macrocyclization reactions affording the AE-C[4]P scaffolds. We hope that this Account will inspire researchers to develop new constructs based on C[4]Ps and apply them in other complementary areas, such as supramolecular catalysis, chemical biology, and materials science.

AUTHOR INFORMATION

Corresponding Authors

Luis Escobar – *The Barcelona Institute of Science and Technology (BIST), Institute of Chemical Research of Catalonia (ICIQ), 43007 Tarragona, Spain; orcid.org/0000-0003-0392-8245; Email: luisescobar1992@hotmail.es*

Qingqing Sun – *The Barcelona Institute of Science and Technology (BIST), Institute of Chemical Research of Catalonia (ICIQ), 43007 Tarragona, Spain; School of Chemistry and Chemical Engineering, Yangzhou University, Yangzhou 225002 Jiangsu, China; Email: sunqingqing@snnu.edu.cn*

Pablo Ballester – *The Barcelona Institute of Science and Technology (BIST), Institute of Chemical Research of Catalonia (ICIQ), 43007 Tarragona, Spain; ICREA, 08010 Barcelona, Spain; orcid.org/0000-0001-8377-6610; Email: pballester@iciq.es*

Complete contact information is available at:

<https://pubs.acs.org/10.1021/acs.accounts.2c00839>

Notes

The authors declare no competing financial interest.

Biographies

Luis Escobar obtained his Ph.D. in 2019 from the University of Rovira and Virgili (URV) and the Institute of Chemical Research of Catalonia (ICIQ) with Prof. Pablo Ballester. After that, he worked as a postdoctoral fellow with Prof. Thomas Carell at the Ludwig Maximilian University (LMU) of Munich. Currently, he is a research associate in the group of Prof. Christopher A. Hunter at the University of Cambridge.

Qingqing Sun received her Ph.D. in 2021 from the URV and the ICIQ with Prof. Pablo Ballester. Currently, she is a Lecturer in the School of Chemistry and Chemical Engineering of Yangzhou University.

Pablo Ballester completed his Ph.D. in 1986 with Prof. Ramon Mestres at the University of the Balearic Islands (UIB). He worked as a postdoctoral fellow with Prof. Julius Rebek, Jr., at the University of Pittsburgh and the Massachusetts Institute of Technology (MIT), and with Prof. José M. Saá at the UIB. In 1990, he joined the Chemistry Department of UIB and went through the ranks of Assistant and Associate Professor. In 2004, he was awarded with an ICREA Research Professorship and moved to Tarragona as ICIQ group leader.

ACKNOWLEDGMENTS

We thank Gobierno de España MICIN/AEI/FEDER, UE (projects CTQ2017-84319-P, PID2020-114020GB-I00 and CEX2019-000925-S), the CERCA Programme/Generalitat de Catalunya, AGAUR (2017 SGR 1123 and 2021 SGR 00851), and the ICIQ Foundation for continued financial support of our research.

REFERENCES

- (1) Adriaenssens, L.; Gil-Ramírez, G.; Frontera, A.; Quiñonero, D.; Escudero-Adán, E. C.; Ballester, P. Thermodynamic Characterization of Halide-π Interactions in Solution Using “Two-Wall” Aryl Extended Calix[4]pyrroles as Model System. *J. Am. Chem. Soc.* **2014**, *136*, 3208–3218.
- (2) Escobar, L.; Ballester, P. Quantification of the hydrophobic effect using water-soluble super aryl-extended calix[4]pyrroles. *Org. Chem. Front.* **2019**, *6*, 1738–1748.
- (3) Sierra, A. F.; Hernández-Alonso, D.; Romero, M. A.; González-Delgado, J. A.; Pischel, U.; Ballester, P. Optical Supramolecular Sensing of Creatinine. *J. Am. Chem. Soc.* **2020**, *142*, 4276–4284.
- (4) Sun, Q.; Escobar, L.; Ballester, P. Hydrolysis of Aliphatic Bisisonitriles in the Presence of a Polar Super Aryl-Extended Calix[4]-pyrrole Container. *Angew. Chem., Int. Ed.* **2021**, *60*, 10359–10365.
- (5) Escobar, L.; Ballester, P. Molecular Recognition in Water Using Macrocyclic Synthetic Receptors. *Chem. Rev.* **2021**, *121*, 2445–2514.
- (6) Houk, K. N.; Leach, A. G.; Kim, S. P.; Zhang, X. Binding Affinities of Host–Guest, Protein–Ligand, and Protein–Transition-State Complexes. *Angew. Chem., Int. Ed.* **2003**, *42*, 4872–4897.
- (7) Persch, E.; Dumele, O.; Diederich, F. Molecular Recognition in Chemical and Biological Systems. *Angew. Chem., Int. Ed.* **2015**, *54*, 3290–3327.
- (8) Hunter, C. A. Quantifying Intermolecular Interactions: Guidelines for the Molecular Recognition Toolbox. *Angew. Chem., Int. Ed.* **2004**, *43*, 5310–5324.
- (9) Pinalli, R.; Dalcanale, E. Supramolecular Sensing with Phosphonate Cavitands. *Acc. Chem. Res.* **2013**, *46*, 399–411.
- (10) Kim, S. K.; Sessler, J. L. Calix[4]pyrrole-Based Ion Pair Receptors. *Acc. Chem. Res.* **2014**, *47*, 2525–2536.
- (11) Kim, D. S.; Sessler, J. L. Calix[4]pyrroles: versatile molecular containers with ion transport, recognition, and molecular switching functions. *Chem. Soc. Rev.* **2015**, *44*, 532–546.
- (12) Yu, Y.; Rebek, J. Reactions of Folded Molecules in Water. *Acc. Chem. Res.* **2018**, *51*, 3031–3040.
- (13) Morimoto, M.; Bierschenk, S. M.; Xia, K. T.; Bergman, R. G.; Raymond, K. N.; Toste, F. D. Advances in supramolecular host-mediated reactivity. *Nat. Catal.* **2020**, *3*, 969–984.
- (14) Ji, X.; Chi, X.; Ahmed, M.; Long, L.; Sessler, J. L. Soft Materials Constructed Using Calix[4]pyrrole- and “Texas-Sized” Box-Based Anion Receptors. *Acc. Chem. Res.* **2019**, *52*, 1915–1927.
- (15) Kohnke, F. H. Calixpyrroles: from Anion Ligands to Potential Anticancer Drugs. *Eur. J. Org. Chem.* **2020**, 4261–4272.
- (16) Yang, L.-P.; Wang, X.; Yao, H.; Jiang, W. Naphthotubes: Macrocyclic Hosts with a Biomimetic Cavity Feature. *Acc. Chem. Res.* **2020**, *53*, 198–208.
- (17) Dong, J.; Davis, A. P. Molecular Recognition Mediated by Hydrogen Bonding in Aqueous Media. *Angew. Chem., Int. Ed.* **2021**, *60*, 8035–8048.
- (18) Baeyer, A. Ueber ein Condensationsproduct von Pyrrol mit Aceton. *Ber. Dtsch. Chem. Ges.* **1886**, *19*, 2184–2185.
- (19) Gale, P. A.; Sessler, J. L.; Král, V.; Lynch, V. Calix[4]pyrroles: Old Yet New Anion-Binding Agents. *J. Am. Chem. Soc.* **1996**, *118*, 5140–5141.
- (20) Custelcean, R.; Delmau, L. H.; Moyer, B. A.; Sessler, J. L.; Cho, W.-S.; Gross, D.; Bates, G. W.; Brooks, S. J.; Light, M. E.; Gale, P. A. Calix[4]pyrrole: An Old yet New Ion-Pair Receptor. *Angew. Chem., Int. Ed.* **2005**, *44*, 2537–2542.
- (21) Gross, D. E.; Schmidtchen, F. P.; Antonius, W.; Gale, P. A.; Lynch, V. M.; Sessler, J. L. Cooperative Binding of Calix[4]pyrrole–

- Anion Complexes and Alkylammonium Cations in Halogenated Solvents. *Chem. Eur. J.* **2008**, *14*, 7822–7827.
- (22) Allen, W. E.; Gale, P. A.; Brown, C. T.; Lynch, V. M.; Sessler, J. L. Binding of Neutral Substrates by Calix[4]pyrroles. *J. Am. Chem. Soc.* **1996**, *118*, 12471–12472.
- (23) Kim, S. K.; Sessler, J. L. Ion pair receptors. *Chem. Soc. Rev.* **2010**, *39*, 3784–3809.
- (24) Bruno, G.; Cafeo, G.; Kohnke, F. H.; Nicolò, F. Tuning the anion binding properties of calixpyrroles by means of *p*-nitrophenyl substituents at their *meso*-positions. *Tetrahedron* **2007**, *63*, 10003–10010.
- (25) Anzenbacher, P., Jr.; Jursíková, K.; Lynch, V. M.; Gale, P. A.; Sessler, J. L. Calix[4]pyrroles Containing Deep Cavities and Fixed Walls. Synthesis, Structural Studies, and Anion Binding Properties of the Isomeric Products Derived from the Condensation of *p*-Hydroxyacetophenone and Pyrrole. *J. Am. Chem. Soc.* **1999**, *121*, 11020–11021.
- (26) Bonomo, L.; Solari, E.; Toraman, G.; Scopelliti, R.; Floriani, C.; Latronico, M. A cylindrical cavity with two different hydrogen-binding boundaries: the calix[4]arene skeleton screwed onto the *meso*-positions of the calix[4]pyrrole. *Chem. Commun.* **1999**, 2413–2414.
- (27) Guinovart, T.; Hernández-Alonso, D.; Adriaenssens, L.; Blondeau, P.; Martínez-Belmonte, M.; Rius, F. X.; Andrade, F. J.; Ballester, P. Recognition and Sensing of Creatinine. *Angew. Chem., Int. Ed.* **2016**, *55*, 2435–2440.
- (28) Hernández-Alonso, D.; Zankowski, S.; Adriaenssens, L.; Ballester, P. Water-soluble aryl-extended calix[4]pyrroles with unperturbed aromatic cavities: synthesis and binding studies. *Org. Biomol. Chem.* **2015**, *13*, 1022–1029.
- (29) Díaz-Moscoso, A.; Hernández-Alonso, D.; Escobar, L.; Arroyave, F. A.; Ballester, P. Stereoselective Synthesis of Lower and Upper Rim Functionalized Tetra- α Isomers of Calix[4]pyrroles. *Org. Lett.* **2017**, *19*, 226–229.
- (30) Galán, A.; Aragay, G.; Ballester, P. A chiral “Siamese-Twin” calix[4]pyrrole tetramer. *Chem. Sci.* **2016**, *7*, 5976–5982.
- (31) Dăbuleanu, D.; Bauzá, A.; Ortega-Castro, J.; Escudero-Adán, E. C.; Ballester, P.; Frontera, A. Synthesis, X-ray Characterization and Density Functional Theory (DFT) Studies of Two Polymorphs of the $\alpha,\alpha,\alpha,\alpha$, Isomer of Tetra-*p*-Iodophenyl Tetramethyl Calix[4]pyrrole: On the Importance of Halogen Bonds. *Molecules* **2020**, *25*, 285.
- (32) During the peer review of our exemplary Account, we became aware of the publication of a comprehensive review on the topic: Rather, I. A.; Danjou, P.-E.; Ali, R. Aryl- and Superaryl-Extended Calix[4]pyrroles: From Syntheses to Potential Applications. *Top. Curr. Chem.* **2023**, *381*, 7.
- (33) Ballester, P. Experimental Quantification of Anion- π Interactions in Solution Using Neutral Host-Guest Model Systems. *Acc. Chem. Res.* **2013**, *46*, 874–884.
- (34) Adriaenssens, L.; Estarellas, C.; Vargas Jentzsch, A.; Martínez Belmonte, M.; Matile, S.; Ballester, P. Quantification of Nitrate- π Interactions and Selective Transport of Nitrate Using Calix[4]pyrroles with Two Aromatic Walls. *J. Am. Chem. Soc.* **2013**, *135*, 8324–8330.
- (35) Kim, A.; Ali, R.; Park, S. H.; Kim, Y.-H.; Park, J. S. Probing and evaluating anion- π interaction in *meso*-dinitrophenyl functionalized calix[4]pyrrole isomers. *Chem. Commun.* **2016**, *52*, 11139–11142.
- (36) Gil-Ramírez, G.; Escudero-Adán, E. C.; Benet-Buchholz, J.; Ballester, P. Quantitative Evaluation of Anion- π Interactions in Solution. *Angew. Chem., Int. Ed.* **2008**, *47*, 4114–4118.
- (37) Camiolo, S.; Gale, P. A. Fluoride recognition in ‘super-extended cavity’ calix[4]pyrroles. *Chem. Commun.* **2000**, 1129–1130.
- (38) Verdejo, B.; Gil-Ramírez, G.; Ballester, P. Molecular Recognition of Pyridine N-Oxides in Water Using Calix[4]pyrrole Receptors. *J. Am. Chem. Soc.* **2009**, *131*, 3178–3179.
- (39) Escobar, L.; Díaz-Moscoso, A.; Ballester, P. Conformational selectivity and high-affinity binding in the complexation of *N*-phenyl amides in water by a phenyl extended calix[4]pyrrole. *Chem. Sci.* **2018**, *9*, 7186–7192.
- (40) Peñuelas-Haro, G.; Ballester, P. Efficient hydrogen bonding recognition in water using aryl-extended calix[4]pyrrole receptors. *Chem. Sci.* **2019**, *10*, 2413–2423.
- (41) Ciardi, M.; Tancini, F.; Gil-Ramírez, G.; Escudero Adán, E. C.; Massera, C.; Dalcanale, E.; Ballester, P. Switching from Separated to Contact Ion-Pair Binding Modes with Diastereomeric Calix[4]pyrrole Bis-phosphonate Receptors. *J. Am. Chem. Soc.* **2012**, *134*, 13121–13132.
- (42) Ciardi, M.; Galán, A.; Ballester, P. Tetra-phosphonate Calix[4]-pyrrole Cavitands as Multitopic Receptors for the Recognition of Ion Pairs. *J. Am. Chem. Soc.* **2015**, *137*, 2047–2055.
- (43) Martínez-Crespo, L.; Sun-Wang, J. L.; Sierra, A. F.; Aragay, G.; Errasti-Murugarren, E.; Bartoccioni, P.; Palacín, M.; Ballester, P. Facilitated Diffusion of Proline across Membranes of Liposomes and Living Cells by a Calix[4]pyrrole Cavitand. *Chem.* **2020**, *6*, 3054–3070.
- (44) Escobar, L.; Aragay, G.; Ballester, P. Super Aryl-Extended Calix[4]pyrroles: Synthesis, Binding Studies, and Attempts To Gain Water Solubility. *Chem. Eur. J.* **2016**, *22*, 13682–13689.
- (45) Lai, Z.; Zhao, T.; Sessler, J. L.; He, Q. Bis-Calix[4]pyrroles: Preparation, structure, complexation properties and beyond. *Coord. Chem. Rev.* **2020**, *425*, 213528.
- (46) Valderrey, V.; Escudero-Adán, E. C.; Ballester, P. Polyatomic Anion Assistance in the Assembly of [2]Pseudorotaxanes. *J. Am. Chem. Soc.* **2012**, *134*, 10733–10736.
- (47) Molina-Muriel, R.; Aragay, G.; Escudero-Adán, E. C.; Ballester, P. Switching from Negative-Cooperativity to No-Cooperativity in the Binding of Ion-Pair Dimers by a Bis(calix[4]pyrrole) Macrocycle. *J. Org. Chem.* **2018**, *83*, 13507–13514.
- (48) He, Q.; Kelliher, M.; Bähring, S.; Lynch, V. M.; Sessler, J. L. A Bis-calix[4]pyrrole Enzyme Mimic That Constrains Two Oxoanions in Close Proximity. *J. Am. Chem. Soc.* **2017**, *139*, 7140–7143.
- (49) Xiong, S.; Chen, F.; Zhao, T.; Li, A.; Xu, G.; Sessler, J. L.; He, Q. Selective Inclusion of Fluoride within the Cavity of a Two-Wall Bis-calix[4]pyrrole. *Org. Lett.* **2020**, *22*, 4451–4455.
- (50) Valderrey, V.; Escudero-Adán, E. C.; Ballester, P. Highly Cooperative Binding of Ion-Pair Dimers and Ion Quartets by a Bis(calix[4]pyrrole) Macrotricyclic Receptor. *Angew. Chem., Int. Ed.* **2013**, *52*, 6898–6902.
- (51) Ballester, P. Supramolecular Capsules Derived from Calixpyrrole Scaffolds. *Isr. J. Chem.* **2011**, *51*, 710–724.
- (52) Adriaenssens, L.; Ballester, P. Hydrogen bonded supramolecular capsules with functionalized interiors: the controlled orientation of included guests. *Chem. Soc. Rev.* **2013**, *42*, 3261–3277.
- (53) Verdejo, B.; Rodríguez-Llansola, F.; Escuder, B.; Miravet, J. F.; Ballester, P. Sodium and pH responsive hydrogel formation by the supramolecular system calix[4]pyrrole derivative/tetramethylammonium cation. *Chem. Commun.* **2011**, *47*, 2017–2019.
- (54) Shimizu, K. D.; Rebek, J. Synthesis and assembly of self-complementary calix[4]arenes. *Proc. Natl. Acad. Sci. U.S.A.* **1995**, *92*, 12403–12407.
- (55) Mogck, O.; Paulus, E. F.; Böhmer, V.; Thondorf, I.; Vogt, W. Hydrogen-bonded dimers of tetraurea calix[4]arenes: unambiguous proof by single crystal X-ray analysis. *Chem. Commun.* **1996**, 2533–2534.
- (56) Mogck, O.; Böhmer, V.; Vogt, W. Hydrogen Bonded Homo- and Heterodimers of Tetra Urea Derivatives of Calix[4]arenes. *Tetrahedron* **1996**, *52*, 8489–8496.
- (57) Ballester, P.; Gil-Ramírez, G. Self-assembly of dimeric tetraurea calix[4]pyrrole capsules. *Proc. Natl. Acad. Sci. U.S.A.* **2009**, *106*, 10455–10459.
- (58) Gil-Ramírez, G.; Chas, M.; Ballester, P. Selective Pairwise Encapsulation Using Directional Interactions. *J. Am. Chem. Soc.* **2010**, *132*, 2520–2521.
- (59) Galán, A.; Valderrey, V.; Ballester, P. Ordered co-encapsulation of chloride with polar neutral guests in a tetraurea calix[4]pyrrole dimeric capsule. *Chem. Sci.* **2015**, *6*, 6325–6333.
- (60) Galán, A.; Escudero-Adán, E. C.; Ballester, P. Template-directed self-assembly of dynamic covalent capsules with polar interiors. *Chem. Sci.* **2017**, *8*, 7746–7750.

- (61) Mirabella, C. F. M.; Aragay, G.; Ballester, P. Influence of the solvent in the self-assembly and binding properties of [1 + 1] tetra-imine bis-calix[4]pyrrole cages. *Chem. Sci.* **2023**, *14*, 186–195.
- (62) Escobar, L.; Villarón, D.; Escudero-Adán, E. C.; Ballester, P. A mono-metallic Pd(II)-cage featuring two different polar binding sites. *Chem. Commun.* **2019**, *55*, 604–607.
- (63) Escobar, L.; Escudero-Adán, E. C.; Ballester, P. Guest Exchange Mechanisms in Mono-Metallic Pd^{II}/Pt^{II}-Cages Based on a Tetra-Pyridyl Calix[4]pyrrole Ligand. *Angew. Chem., Int. Ed.* **2019**, *58*, 16105–16109.
- (64) Sun, Q.; Escobar, L.; de Jong, J.; Ballester, P. Self-assembly of a water-soluble endohedrally functionalized coordination cage including polar guests. *Chem. Sci.* **2021**, *12*, 13469–13476.
- (65) Xie, L.; Zheng, Z.; Lin, Q.; Zhou, H.; Ji, X.; Sessler, J. L.; Wang, H. Calix[4]pyrrole-based Crosslinked Polymer Networks for Highly Effective Iodine Adsorption from Water. *Angew. Chem., Int. Ed.* **2022**, *61*, e202113724.
- (66) Chen, D.; Luo, D.; He, Y.; Tian, J.; Yu, Y.; Wang, H.; Sessler, J. L.; Chi, X. Calix[4]pyrrole-Based Azo-Bridged Porous Organic Polymer for Bromine Capture. *J. Am. Chem. Soc.* **2022**, *144*, 16755–16760.

□ Recommended by ACS

1,2,5-Trimethylpyrrolyl Phosphines: A Class of Strongly Donating Arylphosphines

Janina A. Werra, Fabian Dielmann, et al.

MARCH 19, 2023

ORGANOMETALLICS

READ ↗

Tunable and Switchable Catalysis Enabled by Cation-Controlled Gating with Crown Ether Ligands

Sebastian Acosta-Calle and Alexander J. M. Miller

MARCH 28, 2023

ACCOUNTS OF CHEMICAL RESEARCH

READ ↗

Dehydrogenative Syntheses of Biazoles via a “Pre-Join” Approach

Tianyang Yu, Hao Wei, et al.

JANUARY 11, 2023

JACS AU

READ ↗

TEtraQuinolines: A Missing Link in the Family of Porphyrinoid Macrocycles

Wei Xu, Naoya Kumagai, et al.

JANUARY 23, 2023

JOURNAL OF THE AMERICAN CHEMICAL SOCIETY

READ ↗

Get More Suggestions >